14 April 1994

PHYSICS LETTERS B

ELSEVIER

Physics Letters B 325 (1994) 45–50

Scaling in Steiner random surfaces

C.F. Baillie

Department of Computer Science, University of Colorado Boulder, CO 80309, USA

A. Irbäck

Department of Theoretical Physics, University of Lund, Sölvegatan 14A, S-223 62 Lund, Sweden

W. Janke

Institut fur Physik, Johannes Gutenberg Universitat, D 55099 Mainz, Germany

D.A. Johnston

LPTHE, Universite Paris Sud, Batiment 211, F-91405 Orsay, France [1]

Received 2 December 1993; revised manuscript received 20 January 1994
Editor: P.V. Landshoff

Abstract

It has been suggested that the modified Steiner action functional has desirable properties for a random surface action. In this paper we investigate the scaling of the string tension and massgap in a variant of this action on dynamically triangulated random surfaces and compare the results with the gaussian plus extrinsic curvature actions that have been used previously.

1. Introduction

The issue of whether a non-trivial continuum limit exists for gaussian plus extrinsic curvature (GPEC) lattice actions of the form

$$S = \sum_{\langle ij \rangle} (\boldsymbol{X}_i - \boldsymbol{X}_j)^2 + \lambda \sum_{\Delta_i, \Delta_j} (1 - \boldsymbol{n}_i \cdot \boldsymbol{n}_j) \qquad (1)$$

on dynamically triangulated random surfaces, is of interest for the construction of well-defined lattice versions of string theory [1–5] as well as for constructing models of membranes in biophysics and chemistry. The second term in Eq. (1), where the $\boldsymbol{n}_i$ are the unit normals on neighbouring triangles, is a discretization of the extrinsic curvature and acts as a "stiffness" term. If this term is absent one has a gaussian discretization of the basic Polyakov action [6] which gives rise to pathologically crumpled surfaces due to the failure of the string tension to scale [7]. The dynamical nature of the triangulation is manifested as a sum over triangulations, $\sum_T$, in the canonical (fixed number of points) partition function

$$Z_N(\lambda) = \sum_T \int \prod_{i=1}^{N} d\boldsymbol{X}_i \delta(\sum_i \boldsymbol{X}_i) \exp(-S) \qquad (2)$$

where the delta function is inserted to kill the translational zero-mode, and N is the number of points. This means that we have in effect a fluid surface. The

[1] Address: Sept. 1993–1994, Permanent address: Maths Dept, Heriot-Watt University, Edinburgh, Scotland.

SSDI 0370-2693(94)00220-2

GPEC model of Eqs. (1,2) apparently has a low λ crumpled phase and a large λ smooth phase similar to those displayed by identical models on fixed triangulation surfaces [8] where the sum over triangulations in Eq. (2) is dropped. The initial work in [1] found a pseudo-second order transition on small lattices, but later work [2,4,5] with larger lattices and better statistics suggested rather that the transition was higher order, or a crossover phenomenon [5,9].

The strongest evidence so far that there *is*, indeed, a transition comes from the measurements of the scaling of the string tension and mass gap carried out in [2]. An earlier measurement of the string tension also found results that were consistent with scaling, but in this the points on the boundary, which constituted a large proportion of the total number of points, were physically pinned down [3] and the vanishing of the lattice string tension at the critical point was assumed. Although analytical calculations suggested [10] that the extrinsic curvature coupling λ in Eq. (1) was asymptotically free and hence that there was no non-trivial theory for finite λ in the lattice action, the measurements in [2] were strongly indicative of scaling and hence a finite string tension in physical units. This implies a non-trivial continuum limit at finite λ.

Pending clarification of the behaviour of the GPEC action on dynamical triangulations, we thought it a worthwhile exercise to investigate possible alternative lattice random surface actions in order to see if their behaviour was more (or less!) clear-cut. We have already conducted some preliminary simulations [11,12] of actions containing terms of the form suggested by Savvidy et al. [13,14] that incorporate the modified Steiner functional [15]. The basic "Steiner" action is just

$$S_{\text{Steiner}} = \frac{1}{2}\sum_{\langle ij\rangle} |\boldsymbol{X}_i - \boldsymbol{X}_j|\theta(\alpha_{ij}), \tag{3}$$

where $\theta(\alpha_{ij}) = |\pi - \alpha_{ij}|$ and α_{ij} is the angle between the embedded neighbouring triangles with common link $\langle ij\rangle$. This is essentially a coarse discretization of the absolute value of the trace of the second fundamental form of the surface, rather than its square which appears in the GPEC action. It was observed in [16] that an action containing only this term ran into problems with the entropy of vertices in smooth configurations and failed to give a well-defined grand canonical (varying number of vertices) partition function. It is a relatively simple matter however to concoct variations on this theme that constrain the errant planar vertices somewhat such as

$$S_1 = \frac{1}{2}\sum_{\langle ij\rangle} |\boldsymbol{X}_i - \boldsymbol{X}_j| + \frac{\lambda}{2}\sum_{\langle ij\rangle} |\boldsymbol{X}_i - \boldsymbol{X}_j|\theta(\alpha_{ij}) \tag{4}$$

or even

$$S_2 = \sum_{\Delta} |\Delta| + \frac{\lambda}{2}\sum_{\langle ij\rangle} |\boldsymbol{X}_i - \boldsymbol{X}_j|\theta(\alpha_{ij}), \tag{5}$$

where the $|\Delta|$ is just the area of triangle Δ as seen in the space in which the surface is embedded. In [14] another alternative was suggested in which θ was modified to $\theta(\alpha_{ij}) = |\pi - \alpha_{ij}|^{\xi}$ with $\xi < 1$ which also appeared to improve the convergence of the grand-canonical partition function.

In [11] we carried out simulations of S_1, S_2 along with a further permutation combining a gaussian term with the Steiner part

$$S_3 = \frac{1}{2}\sum_{\langle ij\rangle} (\boldsymbol{X}_i - \boldsymbol{X}_j)^2 + \frac{\lambda}{2}\sum_{\langle ij\rangle} |\boldsymbol{X}_i - \boldsymbol{X}_j|\theta(\alpha_{ij}) \tag{6}$$

and found rather similar behaviour to that seen for the GPEC action on small (72 and 144 nodes) meshes - namely peaks in the specific heats for the respective actions. For S_1 we have

$$C = \frac{\lambda^2}{N}\left(\langle S^2_{\text{Steiner}}\rangle - \langle S_{\text{Steiner}}\rangle^2\right). \tag{7}$$

We also see, by visual inspection of the surfaces, a low λ crumpled phase and a large λ smooth phase. Although the gyration radius, a measure of the size of the embedded surfaces,

$$X2 = \frac{1}{9N(N-1)}\sum_{ij} (\boldsymbol{X}_i - \boldsymbol{X}_j)^2 q_i q_j \tag{8}$$

where the q_i are the number of neighbours of point i, was not monotone increasing with λ as for the GPEC action this could be explained by noting that the Steiner term, unlike the extrinsic curvature, was dimensionful.

2. Expected scaling properties

Our simulations described above were carried out on boundaryless surfaces with spherical topology. The simulations of [2], which were the most convincing demonstration to date of a non-trivial continuum limit, required surfaces with boundaries in order to carry out the scaling measurements of the string tension and mass-gap. These are constructed in an ingenious manner using twisted boundary conditions on a torus, which we now outline, in order to avoid pinning down a disproportionately large amount of lattice at the boundary loops or points. It was observed in [2] that on a torus the sum of vectors X_{ij} along the edges of the triangulation on a closed path could take the values

$$E(n_1, n_2) = n_1 E_1 + n_2 E_2 \tag{9}$$

where the vectors E_1, E_2 are constant and the integers n_1, n_2 denote how many times the path winds round the two respective periods of the torus. For non-zero E_i this means that

$$X_i(k_1, k_2) = X_i + k_1 E_1 + k_2 E_2 \tag{10}$$

where the k_i labelled the particular "copy" of the surface at a given point. The partition function in Eq. (2) is now dependent on the choice of E_i, $Z_N(\lambda) \rightarrow Z_N(\lambda, E_1, E_2)$. Non-zero values of E_1, E_2 correspond to simulating the surface on a frame $E_1 \times E_2$. The important point to note is that it is not necessary to designate any of the points as boundary points in this procedure. It is thus possible to avoid potential poblems with too many points on the boundary for small surfaces.

A canonical string tension $\sigma(\lambda, N, y^2)$ for the system described above is defined by taking $E_1 = (y, 0, 0)$, $E_2 = (0, y, 0)$, $F_N(\lambda, y^2) = -\log Z_N(\lambda, y^2)$ and

$$\sigma(\lambda, N, y^2) = \frac{\partial F_N(\lambda, y^2)}{\partial y^2} \tag{11}$$

where the translational invariance of Z_N means it depends on only the projected area y^2. Similarly a canonical massgap is defined by choosing $E_1 = (y, 0, 0)$, $E_2 = (0, 0, 0)$ and

$$m(\lambda, N, y) = \frac{\partial F_N(\lambda, y)}{\partial y}. \tag{12}$$

It is expected that the N and y^2 dependence in the string tension appears as the ratio $r = y^2/N$ and in the massgap as the ratio $t = y/N$.

It is actually more natural to define the physical string tension in a grand canonical ensemble (with a varying number of points) [17], which can be done by taking the Legendre transform of $F_N(\lambda, y^2)$

$$G(\mu, \lambda, y^2) = N\mu + F_N(\lambda, y^2) \tag{13}$$

where μ is the cosmological constant. For large y^2 one expects $G(\mu, \lambda, y^2) \simeq \bar{\sigma}(\lambda, \mu) y^2$ with

$$\bar{\sigma}(\lambda, \mu) = \frac{\partial F_N}{\partial y^2} = \sigma(\lambda, r). \tag{14}$$

The grand canonical $\bar{\sigma}(\lambda, \mu)$ is expected to scale as

$$\bar{\sigma}(\lambda, \mu) \simeq \sigma_0(\lambda) + d(\lambda) \mu_R^{2\nu} \tag{15}$$

where the exponent ν governs the scaling of the physical area $A_{\text{phys}} \simeq \mu_R^{2\nu} y^2$, with $\mu_R = (\mu - \mu_{\text{crit}})$. It is then possible to deduce the expected scaling of the *canonical* $\sigma(\lambda, r)$:

$$\sigma(\lambda, r) \simeq \sigma_0(\lambda) + \sigma_1(\lambda) r^{2\nu/(1-2\nu)}. \tag{16}$$

The physical string tension $\sigma_{\text{phys}} = \bar{\sigma}(\lambda, \mu)/\mu_R^{2\nu}$ will be infinite unless $\sigma_0(\lambda) \simeq (\lambda - \lambda_{\text{crit}})^{\alpha}$ as we approach a critical point at some λ_{crit} and this σ_0 is accessible in a canonical simulation.

It is also possible to play a similar game with the massgap, defining

$$G(\mu, \lambda, y) = N\mu + F_N(\lambda, y) \tag{17}$$

which is expected to behave as $G(\mu, \lambda, y) \simeq \bar{m}(\lambda, \mu) y$ for large y. In this case we have $\bar{m}(\lambda, \mu) \simeq \mu_R^{\nu}$ and

$$m(\lambda, t) \simeq D(\lambda) t^{\nu/(1-\nu)} \tag{18}$$

which is again accessible to a canonical simulation.

3. Numerical simulations and results

In this paper we apply the methods of [2] to analyse the scaling of the massgap and string tension for one of the variant Steiner actions, S_1. This was chosen because the two terms in the action $\frac{1}{2}\sum_{\langle ij \rangle} |X_i^{\mu} -$

$X_j^\mu|$ and $\sum_{\langle ij\rangle}|X_i^\mu - X_j^\mu|\theta(\alpha_{ij})$ have the same scaling dimensions which simplifies somewhat the choice of observables. If we rescale the coordinates $\boldsymbol{X}_i \to y\boldsymbol{X}_i'$ in S_1 we find $S_1(\boldsymbol{X}_i, y) \to yS_1(\boldsymbol{X}_i', 1)$, which means that with the appropriate boundary conditions for the string tension measurements

$$\sigma(\lambda, r) = \frac{\partial F_N(\lambda, r)}{\partial y^2} = \frac{\langle S_1\rangle - 3(N-1)}{2y^2} \tag{19}$$

for a surface with N points embedded in 3 dimensions. If we use the boundary conditions that are appropriate for the massgap measurements we find

$$m(\lambda, r) = \frac{\partial F_N(\lambda, t)}{\partial y} = \frac{\langle S_1\rangle - 3(N-1)}{y}. \tag{20}$$

We thus simply measure the expectation value of the action with the appropriate choice of frame in order to access information about the string tension and massgap scaling.

In addition, we measure the specific heat as defined in Eq. (7) and histogram the output data at the various λ simulated in order to use the multi-histogram method of Ferrenberg and Swendsen [18], which allows one to estimate the density of states and hence the specific heat for arbitrary λ. We also measure the gyration radius, as defined in Eq. (8), but a certain amount of care is needed with this because of the twisted boundary conditions. We choose to measure the $X2$ using only the component transverse to the frame in the string tension measurements to avoid confusion, and the two components transverse to the line separating the pinned points in the case of the massgap measurements. The autocorrelation times for the various observables are calculated in order to ensure that we have reasonable statistics. We also measure the various acceptances for the lattice and X moves to check that the Monte-Carlo algorithm, which we now describe, is behaving reasonably.

In order to achieve a reasonable amount of vectorization in the code 64 systems were simulated in parallel, with measurements being taken after a sufficient number of sweeps were made to allow them to decorrelate. It proved to be convenient to store the link variables $\boldsymbol{X}_{ij}$ rather than the site variables $\boldsymbol{X}_i$ which allows the incorporation of the twisted boundary conditions as $\boldsymbol{X}_{ij} = \boldsymbol{X}_i - \boldsymbol{X}_j + \boldsymbol{E}_{ij}$, where $\boldsymbol{E}_{ij} = n_{ij}^1\boldsymbol{E}_1 + n_{ij}^2\boldsymbol{E}_2$. The integers n_{ij} are non-zero when the link $\langle ij\rangle$ passes from one of the elementary cells in the parameter space (a plane for the torus) to another. Rounding errors during the simulation can be kept under control by using the transformations

$$\begin{aligned}\boldsymbol{X}_i &\to \boldsymbol{X}_i + l_i^1\boldsymbol{E}_1 + l_i^2\boldsymbol{E}_2\\ \boldsymbol{E}_{ij} &\to \boldsymbol{E}_{ij} + l_i^1\boldsymbol{E}_1 + l_i^2\boldsymbol{E}_2 - l_j^1\boldsymbol{E}_1 - l_j^2\boldsymbol{E}_2\end{aligned} \tag{21}$$

where the l's are arbitrary integers to keep the E_{ij}'s from straying.

The sum over lattices is effected by carrying out local flip moves on adjacent triangles, forbidding flips that lead to degenerate triangulations with less than 3 neighbours per point or with 2-loops. With non-trivial boundary conditions the $\boldsymbol{E}_{ij}$ for affected edges must be changed, whereas the $\boldsymbol{X}_i$ are left untouched. The coordinates $\boldsymbol{X}_i$ are updated with a simple Metropolis scheme, which does not affect the non-trivial boundary conditions. In this paper we report on simulations carried out on relatively small surfaces of size 64 and 144 nodes. We have not proceeded to larger surfaces in the current batch of simulations because there is a hidden penalty built into the direct transcription of the Steiner action we have used in S_1, compared with the GPEC action. Namely, the calculation of $\theta(\alpha_{ij})$ requires an inverse trigonometric operation, rather than the simple multiplications involved in calculating $\boldsymbol{n}\cdot\boldsymbol{n}$ in the GPEC action. It might be possible to avoid this in further simulations by using some trigonometric function with the requisite properties for θ ($\theta(2\pi - \alpha) = \theta(\alpha)$, $\theta(\pi) = 0$, $\theta(\alpha) \geq 0$), but this begs the question of universality.

If we now move on to discuss the measurements made for the string tension and massgap with the choice of frames $\boldsymbol{E}_1 = (y, 0, 0)$, $\boldsymbol{E}_2 = (0, y, 0)$ and $\boldsymbol{E}_1 = (y, 0, 0)$, $\boldsymbol{E}_2 = (0, 0, 0)$ respectively, comparison of Fig. 1 for the string tension and Fig. 2 for the massgap with Figs. 6, 7 in the first of [2] reveal striking similarities. Looking at Fig. 1 for the string tension first we see that the data points, as expected, fall on universal curves as a function of r for a given λ until finite size effects set in at small r. Lines are drawn to guide the eye through the points coming from the $N = 64$ (8×8) surface. For large r, just as for the GPEC action, we would expect a λ independent limit which is what is observed. For small r the λ dependence becomes more marked, with the σ values straddling zero as $r \to 0$ on the 8×8 lattice for $\lambda = 3, 4$. On the 12×12

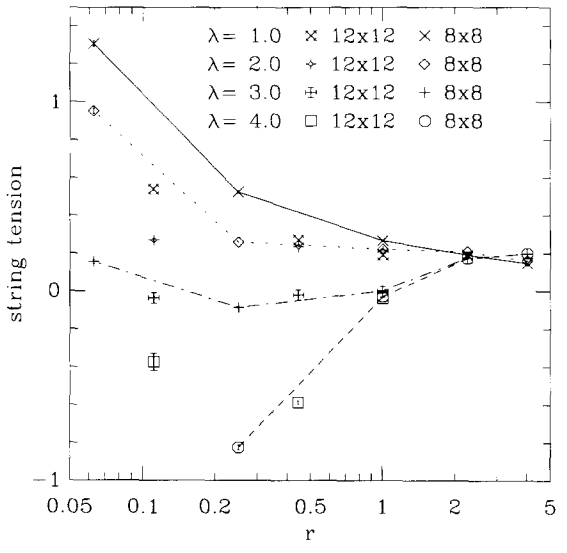

Fig. 1. The canonical string tension $\sigma(\lambda, r)$ is plotted for the various λ values to show the scaling with $r = y^2/N$.

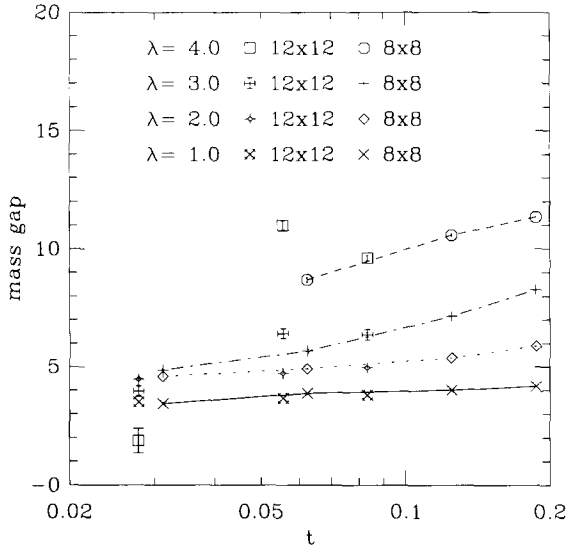

Fig. 2. The canonical massgap $m(\lambda, t)$ is plotted for the various λ to show the scaling with $t = y/N$.

lattice both the results for $\lambda = 3, 4$ lie below the axis which favours a smaller critical coupling. The results suggest that there is some λ_c where $\sigma(\lambda, r) \to 0$ as $\lambda \to \lambda_c$ and $r \to 0$. This is one of the prerequisites for a finite physical string tension. For $\lambda = 4$ we see negative $\sigma(\lambda, r)$ at small r, which is due to the repulsion of the vertices, and the value where it is zero corresponds to the equilibrium configuration. This is again similar to the behaviour observed in the GPEC action, as are the very long autocorrelation times observed in this phase. We would expect the results for $m(\lambda, t)$ in Fig. 2 to fall on universal curves for different λ with $t = y/N$ until finite size effects set in at small t, and this is, indeed, what is seen. We have again drawn lines through the $N = 64$ (8×8) points to guide the eye. No sensible fits to the exponent ν are possible with our data, though Fig. 2 is qualitatively similar to that produced by the GPEC action.

Measurements of $X2$ for the framing used in the string tension measurements appear at first sight to contradict the hypothesis of a smooth phase at large λ as they show a decrease with λ rather than the naively expected increase for sufficiently large frame sizes. However a moments thought suggests that this is, in fact, consistent with a smooth phase as we are only measuring the fluctuations transverse to the frame in $X2$. A typical smooth configuration at large λ will thus be planar and the rigidity will suppress transverse fluctuations and give a small $X2$.

To summarize the numerical results of this paper: for the action S_1, containing an edge length and a Steiner term, the scaling behaviour of both the string tension and the massgap appear similar to those seen in the GPEC action. We do not have enough data at small values of r and t to extract estimates of the exponent ν reliably and check whether they agree, which would be the acid test of scaling. The behaviour of the specific heat peak is consistent with that seen in our earlier, smaller scale, simulations of S_1. Finally $X2$, both with and without framing the surfaces, gives every indication of a smooth or rigid phase at larger λ. There is no sign, however, of sharper scaling behaviour than is seen with GPEC actions, for S_1 at any rate. For future work it is possible that a subdivision invariant action such as S_2 might offer a faster approach to the continuum limit [16]. A more judicious choice of θ from the numerical point of view for any of the Steiner actions S_1, S_2, S_3 might also offer the possibility of more efficient simulations. Nonetheless, the current batch of simulations has demonstrated that there is some evidence for scaling and hence a non-trivial continuum theory for a particular Steiner action, just as with the GPEC action.

4. Acknowledgements

The simulations were carried out on the Cray Y-MP at the San Diego Supercomputer Centre, USA; the Cray Y-MP at the Rutherford Lab, England (SERC grants GR/H 54904 and GR/J 21941); and the Cray Y-MP at HLRZ Jülich, Germany. This work was supported in part by NATO collaborative research grant CRG910091 (CFB and DAJ), and by ARC grant 313-ARC-VI-92/37/scu (WJ and DAJ). CFB was supported by DOE under contract DE-FG02-91ER40672 and by NSF Grand Challenge Applications Group Grant ASC-9217394. WJ thanks the Deutsche Forschungsgemeinschaft for a Heisenberg fellowship. DAJ is supported at LPTHE by an EEC HCM fellowship, an EEC HCM network grant and an Alliance grant.

References

[1] S. Catterall, Phys. Lett. B 220 (1989) 207;
C. Baillie, D. Johnston and R. Williams, Nucl. Phys. B 335 (1990) 469;
C. Baillie, S. Catterall, D. Johnston and R. Williams, Nucl. Phys. B 348 (1991) 543;
S. Catterall, D. Eisenstein, J. Kogut and R. Renken, Nucl. Phys. B 366 (1991) 647.

[2] J. Ambjørn, A. Irbäck, J. Jurkiewicz and B. Petersson, Nucl. Phys. B 393 (1992) 571;
J. Ambjørn, A. Irbäck, S. Varsted, J. Jurkiewicz and B. Petersson, Phys. Lett. B 275 (1992) 295.

[3] S. Catterall, Phys. Lett. B 243 (1990) 127.

[4] M. Bowick, P. Coddington, L. Han, G. Harris and E. Marinari, Nucl. Phys. B 394 (1993) 791.

[5] K. Anagnostopoulos, M. Bowick, P. Coddington, M. Falcioni, L. Han, G. Harris and E. Marinari, "Fluid Random Surfaces with Extrinsic Curvature: II", SU-HEP-93-4241-540, hep-lat/9308091.

[6] A.M. Polyakov, Phys. Lett. B 103 (1981) 207.

[7] J. Ambjørn, B. Durhuus and J. Frohlich, Nucl. Phys. B 257 (1985) 433;
D. Boulatov, V. Kazakov, I Kostov and A. Migdal, Nucl. Phys. B 275 (1986) 641;
A. Billoire and F. David, Nucl. Phys. B 275 (1986) 617;
J. Jurkiewicz, A. Krzywicki and B. Petersson, Phys. Lett. B 168 (1986) 273;
J. Ambjørn, B. Durhuus and J. Frohlich, Nucl. Phys. B 257 (1985) 433;
J. Ambjørn and B. Durhuus, Phys. Lett. B 118 (1987) 253.

[8] Y. Kantor and D. Nelson, Phys. Rev. Lett. 58 (1987) 2774;
J. Ambjørn, B. Durhuus and T. Jonsson, Nucl. Phys. B 316 (1989) 526;
R. Harnish and J. Wheater, Nucl. Phys. B 350 (1993) 447;
J. Wheater and P. Stephenson, Phys. Lett. B 302 (1993) 447.

[9] C. Baillie and D. Johnston, "2d O(3) + 2d QG", hep-lat 9110003. COLO-HEP-324, LPTHE-93-39.

[10] A. Polyakov, Nucl. Phys. B 268 (1986) 406;
H. Kleinert, Phys. Lett. B 174 (1986) 335;
W. Helfrich, J. Phys. 46 (1985) 1263.

[11] C. Baillie, D. Espriu and D. Johnston, Phys. Lett. B 305 (1993) 109.

[12] C.F. Baillie and D.A. Johnston, Phys. Rev. D 45 (1992) 3326.

[13] R. Ambartzumian, G.K. Savvidy, K.G. Savvidy and G. Sukiasian, Phys. Lett. B 275 (1992) 99;
G.K. Savvidy and K.G. Savvidy, Int. J. Mod. Phys. A 8 (1993) 3993.

[14] G.K. Savvidy and K.G. Savvidy, "Gonihedric string and asymptotic freedom", Frankfurt preprint 93-0046, hep-th 9301001.

[15] J. Steiner, Gesammelte Werke Vol. 2, Berlin (1927) 171.

[16] B. Durhuus and T. Jonsson, Phys. Lett. B 297 (1992) 271.

[17] F. David and S. Leibler, J. de Phys. (Paris) II (1991) 959.

[18] A. Ferrenberg and R. Swendsen, Phys. Rev. Lett. 63 (1989) 1195.